



Supramolecular blends of *C*-alkylpyrogallol[4]arenes and polytetrahydrofurans

Oleg Andrew Kulikov ^{a,b,*}, Arshad Mehmood ^c, Sergey Vodzinsky ^d

^a Department of Chemistry, Massachusetts Institute of Technology, Cambridge, MA, 02139, USA

^b Huntsman Advanced Materials, The Woodlands, TX, 77381, USA

^c Department of Chemistry, Texas Christian University, Fort Worth, TX, 76129, USA

^d I. I. Mechnikov Odessa National University, 65000 Odessa, Ukraine

ARTICLE INFO

Keywords:

Supramolecular
Polymers
Pyrogallolarene

ABSTRACT

A small series of the amphiphilic macrocycles – *C*-alkylpyrogallol[4]arenes has been synthesized and examined by single crystal X-ray analysis which showed the formation of two supramolecular arrangements depending on solvent used for crystallization, *i.e.*, multilayered motif and hexameric capsule. Those structural findings provided an insight into blends prepared from aforementioned macrocycles and various polytetrahydrofurans (polyTHFs). Thus, 1:1 wt ratio mixtures were obtained and investigated by combination of Fourier-transform infrared spectroscopy (FT-IR), differential scanning calorimetry (DSC), and thermogravimetric analysis (TGA). As it turned out, the viscosity of these blends was increased compared to starting materials, which imply that pyrogallol[4]arenes can be successfully utilized as supramolecular cross-linkers enhancing H-bonding between adjacent macromolecular chains. As the major difference between compounds synthesized is the length and geometry of their respective alkyl side chains attached directly to macrocyclic core, *i.e.*, *n*-propyl- and cyclohexyl- vs. *n*-dodecyl-, it seemed likely that even insignificant increase in their hydrophobicity can induce high order aggregation of nanoparticles in the slurries, thus affecting their viscosity. Overall, material viscoelastic properties are tunable at macroscopic level by choosing particular pyrogallol[4]arene/solvent combination and adjusting the temperature, which may be advantageous for the design of hybrid materials.

Introduction

Recently, four-fold symmetric OH-containing macrocycles closely related to well-established calixarene family, such as resorcin[4]arenes and pyrogallol[4]arenes, [1–6] have attracted significant attention due to their unique properties making them suitable for diverse applications including removal of lead(II), chromium (II), and copper(II) heavy metal ions through an adsorption process, [7] as antioxidant and UV-B protectors, [8] cobalt-seamed coordination nanocapsule micelles as water reduction catalysts, [9] also evaluated as novel and efficient organo-catalysts for biodiesel production, [10] hosts for neurotransmitters (*e.g.*, choline, betaine, and carnitine) in DMSO and in the gaseous phase, [11] as media for molecular hydrogen storage, [12] antimalarial agents examined through in vitro heme polymerization inhibitory assay, [13] ion transporters through bilayer membranes, [14,15] synthetic ion channels [16] and pores, [17] frustrated organic solids for CO₂ sorption. [18] Also, pyrogallol[4]arenes were investigated for their dispersing

properties with regard to cement particles, [19] successfully used as star-like initiators for the controlled radical polymerization, [20] as well as found to be promising drug delivery platform. [21] Further, a series of straight and branched chain pyrogallol[4]arenes was studied against strains of *E. coli*, [22] and also an oxidative stability of pyrogallol[4] arenes proved them to be effective antioxidants [23] of polymers at temperatures above 150 °C. Finally, the cavity of resorcinarene and pyrogallol[4]arene capsules like nanoreactors was extensively examined in catalysis studies, [24–29] more specifically, in a competitive (chloroform) and non-competitive (benzene) solvents. [30,31] Importantly, electron-rich resorcin[4]arenes can be used as potent anion receptors and transporters. [32] Recent contribution [33] detailed molecular entrapment of commercially available PEG-oligomers by this type of OH-containing macrocycles as a result of intermolecular H-bonding. In general, assembly of such supramolecular architectures can be driven by strong intermolecular H-bonding, π-π stacking, van der Waals, and hydrophobic interactions that may have some practical applications in

* Corresponding author at: Department of Chemistry, Massachusetts Institute of Technology, Cambridge, MA, 02139, USA.

E-mail addresses: Oleg_Kulikov@huntsman.com, okulikov@mit.edu (O. Andrew Kulikov).

developing adhesive materials with predetermined viscosity. In this regard, studies on improved adhesion of polyurethanes to polyesters facilitated by pyrogallol[4]arenes should not be underestimated. [34] Thus, to increase adhesion forces, macrocyclic ligands such as calixarenes, resorcinarenes and pyrogallolarenes, which have two well-separated regions, *i.e.*, hydrophilic and hydrophobic, have been fixed on the surface of polyester fabrics. Also, polyTHFs as toughening modifiers can be utilized to improve thermal and mechanical properties in epoxy resin systems. [35] In addition to that, adhesive strength and rheological characteristics of automotive structural adhesives including polyurethane (PU) toughening agents derived from polyTHF and hexamethylene diisocyanate have been thoroughly investigated. [36] Importantly, relatively low molecular weight polyTHF based polymer ($<2000 \text{ g mol}^{-1}$) exhibited properties typical for high molar mass polymers, *i.e.*, behavior similar to a semi-crystalline material. [37] This is attributed to the presence of the hydrogen bonds, in combination with phase separation giving rise to hard domain formation. Thus, in comparison with a covalently bonded and a low molecular weight material of similar composition, the melamine based polyTHF-urethane supramolecular compounds have a higher and more temperature dependent viscosity. Similar design concept was used to prepare supramolecular polyTHF based on pyrimidinone, [38] when 2-ureido-4[1H]-pyrimidinone terminated polytetrahydrofuran, polyTHF(UPy)₂ was assembled through reversible H-bonding into polymer-like material which behaves like thermoplastic elastomer. The rheological studies revealed that the supramolecular structure of polytetrahydrofuran functionalized with UPy end groups is stable up to 80 °C. Above that temperature the supramolecular architectures started to dissociate, which is indicated by a sharp decrease in material viscosity allowing polyTHF(UPy)₂ material processing. Alternative polytetrahydrofuran structures with one of their end-groups functionalized with a supramolecular entity capable of strong stacking/H-bonding [39] were reported to form the supramolecular mimic for bottlebrush polymers in bulk which appeared to be the good candidates for supersoft elastomers. Also, polyTHFs are used as an effective binder ingredients for improving the performance of propellants. Particularly interesting was viscoelastic behaviour of polyTHF binder prepared employing glycerin as a crosslinking modifier [40].

Herein, we report self-assembly of three pyrogallol[4]arenes, namely, *C*-propyl- (*C*₃-Pg), *C*-cyclohexyl- (Cyclohexyl-Pg), and *C*-dodecylpyrogallol[4]arene (*C*₁₂-Pg) with different polyTHF molecules which may be potentially used to construct various supramolecular arrangements due to their non-covalent interactions. We reasoned that using such calixarene-like macrocyclic scaffolds which bear multiple polar OH-groups may be beneficial to promote intermolecular H-bonding and dipole interactions, thus, resulting in formation of the different Pg@polyTHF compounds. Considering the fact that pyrogallol[4]arenes tend to assemble into either multilayer arrangement, hexameric capsule or nanotubular motif as well as recent assertions [5] that pyrogallolarene capsules can accommodate more solvent molecules relative to their resorcinarene counterparts, we have chosen their polymorphic motifs obtained by crystallization from different solvents as plausible cross-linking factors to manipulate polyTHFs adhesive properties. More

specifically, we utilized polar solvents, such as DMF and a mixture of EtOAc/MeCN (1:1, v) to obtain a multilayer form of *C*₁₂-Pg as well as mixture of PhNO₂/MeOH (10:1, v) to prepare hexameric nanocapsules.

Single crystal X-ray studies of *C*-alkylpyrogallol[4]arenes

To investigate an effect of pyrogallol[4]arenes crystal packing on their interaction with polyTHF molecules of different length, we obtained single crystal X-ray data for two *C*-substituted pyrogallol[4]arenes, *i.e.*, Cyclohexyl-Pg and *C*₁₂-Pg, both crystallized from EtOAc/MeCN (1:1, v) solvent mixture (Fig. 1, 2). Although Cyclohexyl-Pg side chains contain only one extra carbon atom compared to the known 3-pentylpyrogallol[4]arene (Fig. S1), which is prone to self-assemble into channel-like network, it causes dramatic changes in assembly behavior leading to layered arrangements (Figs. S2–S4) reminiscent of the previously reported Cyclohexyl-Pg bilayer [41].

In a similar fashion, crystallization of *C*₁₂-Pg from polar solvents resulted in a variety of layered supramolecular motifs with unremarkable structural differences shown in the Fig. 2 and S5–S16 with solvents EtOAc/MeCN (1:1, v) and DMF, respectively. Alternatively, hexameric nanocapsules were obtained in the solvent mixture of PhNO₂/MeOH (10:1, v), Fig. 3, S17–S20 with a size matching up closely dimensions of similar H-bonded assemblies previously described in the literature [41,42]. Overall, it seemed likely that straight chain pyrogallol[4]arenes are not prone to assemble into nanotubes unlike their synthetic analogue having a branched substitution pattern, *e.g.*, 2-pentylpyrogallol[4]arene [41]. We hypothesize that amphiphilic *C*₁₂-Pg macrocycle having hydrophilic crown and hydrophobic alkyl side arms can be easily blended with a great variety of polyols, such as PEGs or polyTHFs due to the interaction of their respective polar segments.

Generally, in a crystal lattice these species are held together by a network of O-H···O intermolecular hydrogen bonds with the following distances: 2.54–2.65 Å (C₁₂-Pg from DMF) or O-H···O contacts, such as 1.89–3.53 Å (C₁₂-Pg from EtOAc/MeCN), 2.66 Å (Cyclohexyl-Pg), and 2.41–2.98 Å (C₁₂-Pg from PhNO₂/MeOH). All the macrocycles adopted non-planar conformation with four *meso*-substituents projected on one side, thus having configuration of *rccc*-isomer (Fig. S17). Additionally, we discovered that C₁₂-Pg can be assembled into well-known hydrogen-bonded hexameric capsule arrangement with dodecyl chains projected towards periphery when crystallized from PhNO₂/MeOH (10:1, v) mixture, Fig. 3, S17–S20.

Noteworthy, C₁₂-Pg macrocycle tends to form “close-to-spherical” aggregates of nanometer size when deposited either from EtOAc/MeCN (1:1, v), DMF or PhNO₂/MeOH (10:1, v) stock solutions on carbon coated copper grid (Figs. S21, S22) suggestive that its supramolecular organization revealed by single crystal X-ray analysis (*i.e.*, capsular or layered arrangements) may not be directly related to the TEM imaging data. Overall, oxygen-rich pyrogallol[4]arene molecules capable of establishing intermolecular H-bonds and hydrophobic side-chain/side-chain interactions with each other may represent a convenient platform for binding various diol structures, thus enhancing their adhesive properties.

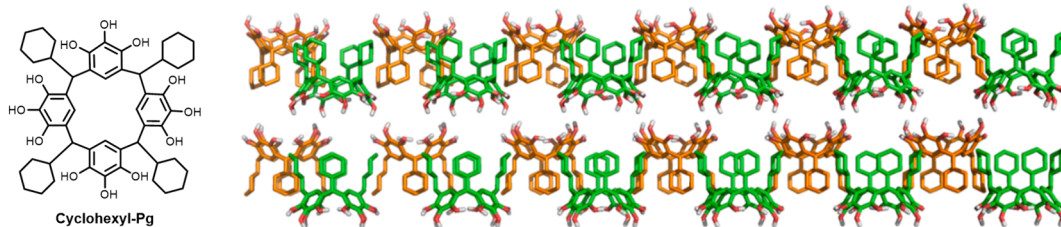


Fig. 1. Partial crystal packing diagram of *C*-cyclohexylpyrogallol[4]arene from EtOAc/MeCN (Cyclohexyl-Pg, CCDC1853364) featuring formation of bilayer arrangement – green and brown color scheme represents oppositely oriented macrocycles (H-atoms of alkyl chains and aromatic segments are omitted for clarity). (For interpretation of the references to color in this figure legend, the reader is referred to the web version of this article.)

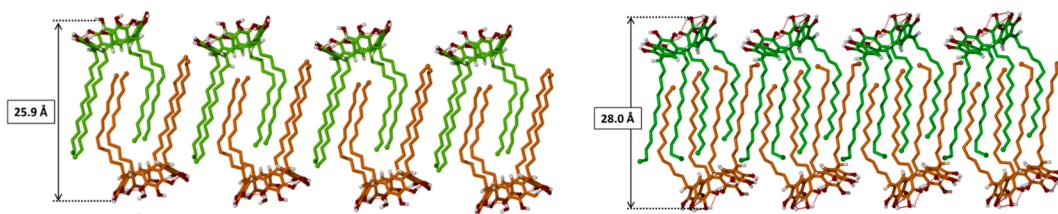


Fig. 2. Partial crystal packing diagram of *C*-dodecylpyrogallol[4]arene, C₁₂-Pg (left stack, CCDC 1868974, from DMF; right stack, CCDC 1868972, from EtOAc/MeCN) featuring formation of bilayer arrangement.

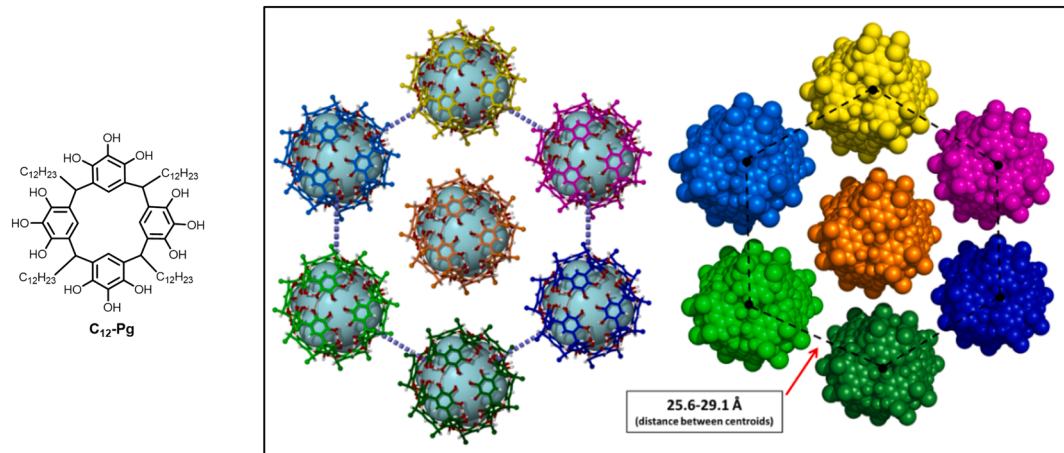


Fig. 3. Partial crystal packing diagram of *C*-dodecylpyrogallol[4]arene, C₁₂-Pg (CCDC 1868973, from PhNO₂/MeOH) featuring formation of hexameric nanocapsules (badly disordered alkyl chains are omitted for clarity).

Formation of supramolecular pyrogallol [4] arene based blends with various polytetrahydrofurans

We hypothesize that OH-groups of pyrogallol[4]arene cavity may interact with polyTHF segments through hydrogen bonding, therefore, influencing ordering of macromolecules and increasing viscosity of the blends. Also, it seemed likely that this phenomenon may depend on a structure of the macrocycle, *i.e.*, type of alkyl substituents appended to pyrogallol[4]arene crown, as well as on the length of polyTHF chain. Rotational viscometer at specific temperatures and shear rate was used to determine the fluid viscosity for the semi-solid C₁₂-Pg@polyTHF blends in solvents like EtOAc, EtOAc/MeCN (1:1, v), DMF, PhNO₂/MeOH (10:1, v) (Table 1). Importantly, sudden drop of viscosity at 50 °C for C₁₂-Pg(bilayer)@polyTHF₁₀₀₀ can be attributed to the overall density (material's thickness) increase for polyTHF₁₀₀₀ derived slurries comparatively to polyTHF₂₅₀ and polyTHF₆₅₀ homologous structures. The latter may result in slurry material's discontinuity during viscosity determination and, therefore, anomalous values.

Polytetrahydrofurans (polyTHFs) are an extremely versatile class of polyether compounds which is widely used as adhesives [43] or adhesive intermediates for PU prepolymer with adjustable cross-linking characteristics and shear viscosity. PolyTHF molecules of different length were selected as model scaffolds with potentially tunable shear viscosity. To explore hydrophilic/hydrophilic interactions of aforementioned pyrogallol[4]arenes with polyTHF_(250, 650, 1000, 2000, 2900) scaffolds, three macrocycles with different peripheral substitution pattern were chosen, *i.e.*, C₃-Pg, C₁₂-Pg, and Cyclohexyl-Pg, correspondingly. The C₁₂-Pg@polyTHF blends are of specific interest to us as they permit two well-separated regimes, *i.e.*, hydrophilic (formed by pyrogallol[4]arene crowns and polyTHF segments) and hydrophobic (formed by interdigitating *n*-C₁₂-chains). The rationale behind our decision is that a type of supramolecular arrangement of C₁₂-Pg macrocycle, *i.e.*, either bilayer motif or hexameric nanocapsule, when mixed

together with specific polyTHF in a particular solvent, such as EtOAc, DMF, or PhNO₂/MeOH (10:1, v) binary mixture, may resemble its respective X-ray pattern. As shown previously, [44] C₁₂-Pg macrocycle formed bilayer type supramolecular arrangement when crystallized from EtOAc, so its X-ray analysis findings may be projected towards C₁₂-Pg macrocycle blends with various polyTHF molecules prepared in the same solvent. Further, layered supramolecular organizations found for C₁₂-Pg in the current research (solvents: EtOAc/MeCN, DMF) may have an effect on composition of their respective polyTHF blends. Thus, measurement of the C₁₂-Pg@polyTHF₂₀₀₀ viscosity revealed evidence for interaction between polyTHF₂₀₀₀ molecules and corresponding C₁₂-Pg macrocycle as determined values (Table 1) are somewhat higher than that of polyTHF₂₀₀₀ starting material. At 100 °C, the viscosity numbers show a general trend to decrease for all the entries regardless of the solvent used indicating the lack of cohesion forces between adjacent polyTHF molecules with temperature. The solvent effect, *i.e.*, switching between DMF, EtOAc, and EtOAc/MeCN for a particular polyTHF, is not that pronounced and marginal differences can be attributed to the temperature fluctuations. We believe that viscosity may be randomly affected by the preparation conditions of mixtures as well as by crystallization process. Presumably, pyrogallol[4]arene molecules either in a form of bilayer or capsule act as supramolecular cross-linkers stitching up the individual polyTHF chains due to extensive OH···O intermolecular bonding. Investigation of bilayer motif for Cyclohexyl-Pg blended with polyTHFs is indicative of the similar trend discussed above (Table S1). There are closely related accounts of the polyTHF viscosity determinations in the literature, such as, methoxy-terminated THF polymers studied in cyclohexane, toluene, THF, methyl ethyl ketone, and cyclohexanone [45]. Also, measurements of the viscosity were performed for polytetrahydrofuran under different conditions of temperature and solvent [46]. It was of interest to compare aforementioned results with findings for C₁₂-Pg crystallized from PhNO₂/MeOH (10:1, v) and mixed with various polyTHFs as this particular solvent mixture

Table 1

Averaged fluid viscosity data (Poise) for C₁₂-Pg macrocycle blended with various polyTHFs in 1:1 wt ratio. Note: all starting polyTHFs are free-flowing liquids at 50, 80, and 100 °C, correspondingly, whereas C₁₂-Pg material appeared to be a crystalline solid in a range of temperatures examined.

C-dodecylpyrogallol[4]arene/ polyTHF (1:1, w/w)	Viscosity, 50 °C (P)	Viscosity, 80 °C (P)	Viscosity, 100 °C (P)
C ₁₂ -Pg(bilayer)@polyTHF ₂₅₀ (EtOAc)	15.6	1.7	1.9
C ₁₂ -Pg(bilayer)@polyTHF ₆₅₀ (EtOAc)	30.8	19.9	12.1
C ₁₂ -Pg(bilayer)@polyTHF ₁₀₀₀ (EtOAc)	30.1	15.7	11.8
C ₁₂ -Pg(bilayer)@polyTHF ₂₀₀₀ (EtOAc)	42.0	10.7	9.7
C ₁₂ -Pg(bilayer)@polyTHF ₂₉₀₀ (EtOAc)	solid	20.4	14.6
C ₁₂ -Pg(bilayer)@polyTHF ₂₅₀ (EtOAc/MeCN)	23.9	3.9	free-flowing liquid
C ₁₂ -Pg(bilayer)@polyTHF ₆₅₀ (EtOAc/MeCN)	24.8	11.5	2.4
C ₁₂ -Pg(bilayer)@polyTHF ₁₀₀₀ (EtOAc/MeCN)	3.9	10.7	4.2
C ₁₂ -Pg(bilayer)@polyTHF ₂₀₀₀ (EtOAc/MeCN)	thick slurry	thick slurry	4.9
C ₁₂ -Pg(bilayer)@polyTHF ₂₉₀₀ (EtOAc/MeCN)	solid	32.7	13.0
C ₁₂ -Pg(bilayer)@polyTHF ₂₅₀ (DMF)	16.9	1.5	free-flowing liquid
C ₁₂ -Pg(bilayer)@polyTHF ₆₅₀ (DMF)	29.3	2.5	1.2
C ₁₂ -Pg(bilayer)@polyTHF ₁₀₀₀ (DMF)	—	13.3	free-flowing liquid
C ₁₂ -Pg(bilayer)@polyTHF ₂₀₀₀ (DMF)	31.1	15.3	2.3
C ₁₂ -Pg(bilayer)@polyTHF ₂₉₀₀ (DMF)	solid	13.7	7.9
C ₁₂ -Pg(caps.)@polyTHF ₂₅₀ (PhNO ₂ /MeOH)	9.6	4.2	1.8
C ₁₂ -Pg(caps.)@polyTHF ₆₅₀ (PhNO ₂ /MeOH)	5.9	1.6	0.8
C ₁₂ -Pg(caps.)@polyTHF ₁₀₀₀ (PhNO ₂ /MeOH)	9.9	2.4	2.3
C ₁₂ -Pg(caps.)@polyTHF ₂₀₀₀ (PhNO ₂ /MeOH)	thick slurry	11.0	11.2
C ₁₂ -Pg(caps.)@polyTHF ₂₉₀₀ (PhNO ₂ /MeOH)	7.3	1.4	liquid
polyTHF ₂₀₀₀₍₂₉₀₀₎	7.7(22.9)	2.8(10.7)	1.6(7.5)

afforded quite stable H-bonded hexameric capsules likely maintaining their integrity even when blended with polyTHFs. It was shown previously that similar hexameric pyrogallol[4]arene based hydrogen-bonded molecular capsules are quite stable in a polar media, such as 1:1 water/acetone mixture, [47] hence, they may not disintegrate in the presence of polyTHF segments. Moreover, such hexameric capsules were found to demonstrate an exceptional kinetic stability [48]. Conversely, the bilayer motif organization may be susceptible to disruption and exists in dynamic equilibrium with individual pyrogallol[4]arene molecules as it was previously outlined for possible association of pyrogallol [4]arenes at the air–water interface [49]. In this context, it is reasonable to assume that relatively long and flexible polyTHF segments (especially, polyTHF_{2000, 2900}) may wrap up an entire C₁₂-Pg nanocapsule (obtained by crystallization in PhNO₂/MeOH, 10:1, v) rather than to be entrapped within capsular cavity. Data analysis (Table 1) suggested close but lower viscosity for C₁₂-Pg(caps.)@polyTHFs compared to C₁₂-Pg(bilayer)@polyTHFs blends, especially at 50 °C. That is due to the specific interactions between thermodynamically stable hexameric nanocapsules and polyTHF macromolecules which may be less efficient compared to individual pyrogallol[4]arene molecules formed as a result of bilayer motif disintegration in the polar medium. We hypothesize that pyrogallol[4]arene monomers offer more easily accessible OH-groups for binding with polyTHF segments, hence, they may act more

efficiently as supramolecular cross-linkers or nucleating sites in the blends compared to capsular hexamers which are less involved in the linking together with the adjacent polyTHF chains. From the data presented in the Tables 1 and S1, it can be seen that viscosity does not vary significantly with the structure of macrocyclic component, i.e., pyrogallol[4]arene substitution pattern. This implies that macrocyclic hydrophobic/hydrophobic side chain interactions (Figs. 1 and 2) may not influence non-covalent bonding of the adjacent polyTHF molecules.

In addition to that, we investigated aforementioned blends with FT-IR analysis. Shown in the upper panel of the Fig. 4 are representative spectra of DMF based blends of C₁₂-Pg(bilayer)@polyTHF_(250, 650, 1000, 2000, 2900). One noticeable difference in profiles compared to C₁₂-Pg starting material is a band at 1653 cm⁻¹ likely attributed to the characteristic absorption of carbonyl group (from residual DMF) which persists in the blend structure even after drying material under high vacuum. It is uncertain at this point if solvate DMF molecules are actually bridging neighboring or opposite C₁₂-Pg crowns (similarly to shown in Figs. S6, S7 of single crystal X-ray diagram) or if they are simply involved in interaction with polyTHF chains.

Likewise, C₁₂-Pg@polyTHF blends obtained in different solvents showed somewhat similar FT-IR features, (Figs. S23–S27) as well as C-propyl- and C-cyclohexylpyrogallol[4]arene based blends when compared to starting materials (Figs. S28–S34). More specifically, the presence of the broad peak (or a group of overlapping peaks) at ~3290 cm⁻¹ may be due to an intermolecular H-bonding, whereas two distinctive bands in the range of ~2860–2930 cm⁻¹ could be assigned to C-H linkage.

To evaluate thermal stability of the polyTHF slurries, we used thermogravimetric analysis (TGA) (Fig. 4, S35–S43 Tables S2–S4). Our major finding for plots displayed in the lower panel of Fig. 4 was that most of the entries (except C₁₂-Pg@polyTHF₂₅₀ compounds) have an onset point at ~386 °C, whereas C-dodecylpyrogallol[4]arene showed two onset points at 288 and 418 °C, respectively. In this context, the plausible explanation of observed experimental data is that DMF based semi-solid compounds are somewhat similar in terms of thermal stability compared to C₁₂-Pg and polyTHF starting materials (Fig. S43), i.e., decomposition and weight loss primarily occurred at temperatures below 450 °C. The rest of C₁₂-Pg based slurries (solvents: PhNO₂/MeOH, EtOAc, and EtOAc/MeCN, Figs. S35–S37) as well as Cyclohexyl-Pg based blends (solvents: MeCN, EtOAc/MeCN, Figs. S39, S40) represent mostly featureless slopes indicative of the same trend, i.e., homogeneity of the material and its relative thermal stability. Conversely, plots displayed in the Figs. S38, S41, S42 look vastly different, i.e. having multiple onset points in their respective profiles (especially, C₃-Pg based blends, Figs. S41, S42) which may be referred to the nucleating and crystallization in semi-solids during sample preparation, thus, causing lack of sample uniformity. The latter may be associated with low solubility of both C₃-Pg and C₁₂-Pg in MeCN. Comparison of C₃-Pg@polyTHF₆₅₀ plots recorded for both deposit and filtrate fractions suggested that MeCN-filtrate contains a large amount of unreacted C₃-Pg starting material (Fig. S42). Predictably, polyTHF₂₅₀ based mixtures demonstrated lower thermal stability than other examined materials. This is not unexpected behavior for the short-chain polyTHF₂₅₀ as its molecules tend to vaporize more easily as temperature increases. Overall, data implied that supramolecular organization of the blends at high temperatures may have a negligible effect on thermal stability of material as the temperatures of 50 % weight loss can occur in a wide range from 283.5 to 404.8 °C regardless of the solvent used (Tables S2–S4).

It was of interest for us to examine the thermal transitions of mixtures formed with DSC technique which revealed multiple phase transitions likely related to the melting points. We presume that polyTHF chains may compete with those of macrocycle for entrapment of the solvent molecules. It seemed very likely that solvents used to crystallize corresponding pyrogallol[4]arene may be partially remained in the slurry material even after drying under high vacuum, that is forming stable solvates, so the release of entrapped solvent at high temperatures

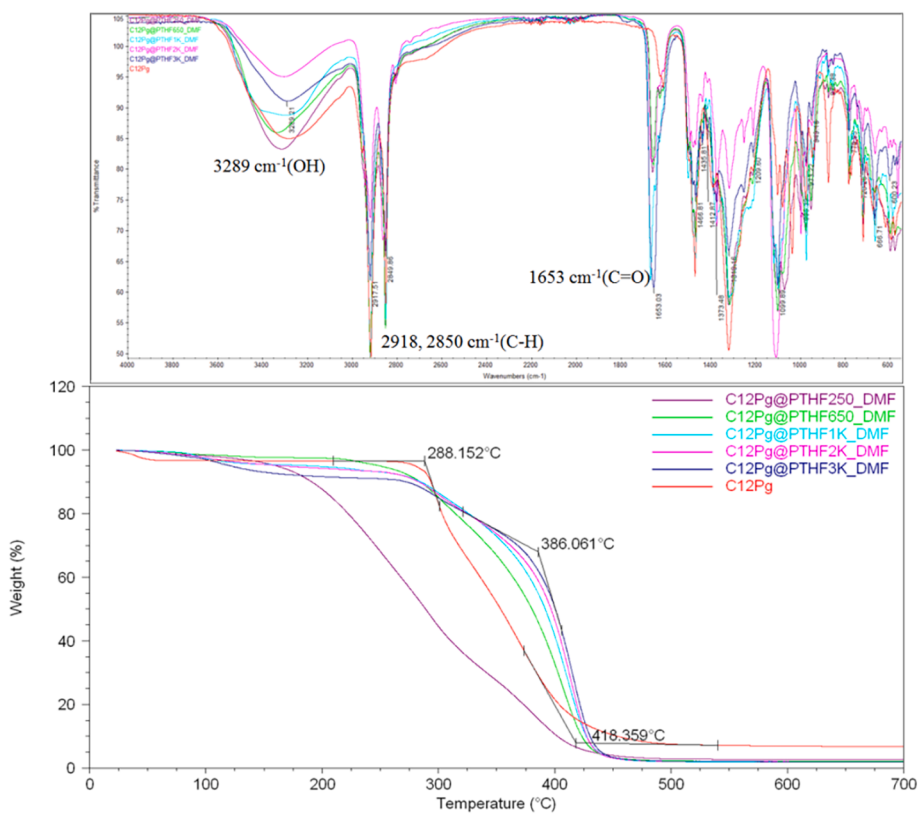


Fig. 4. FT-IR spectra overlay and TGA plots of $\text{C}_{12}\text{-Pg@polyTHF}_{(250, 650, 1000, 2000, 2900)}$ blends.

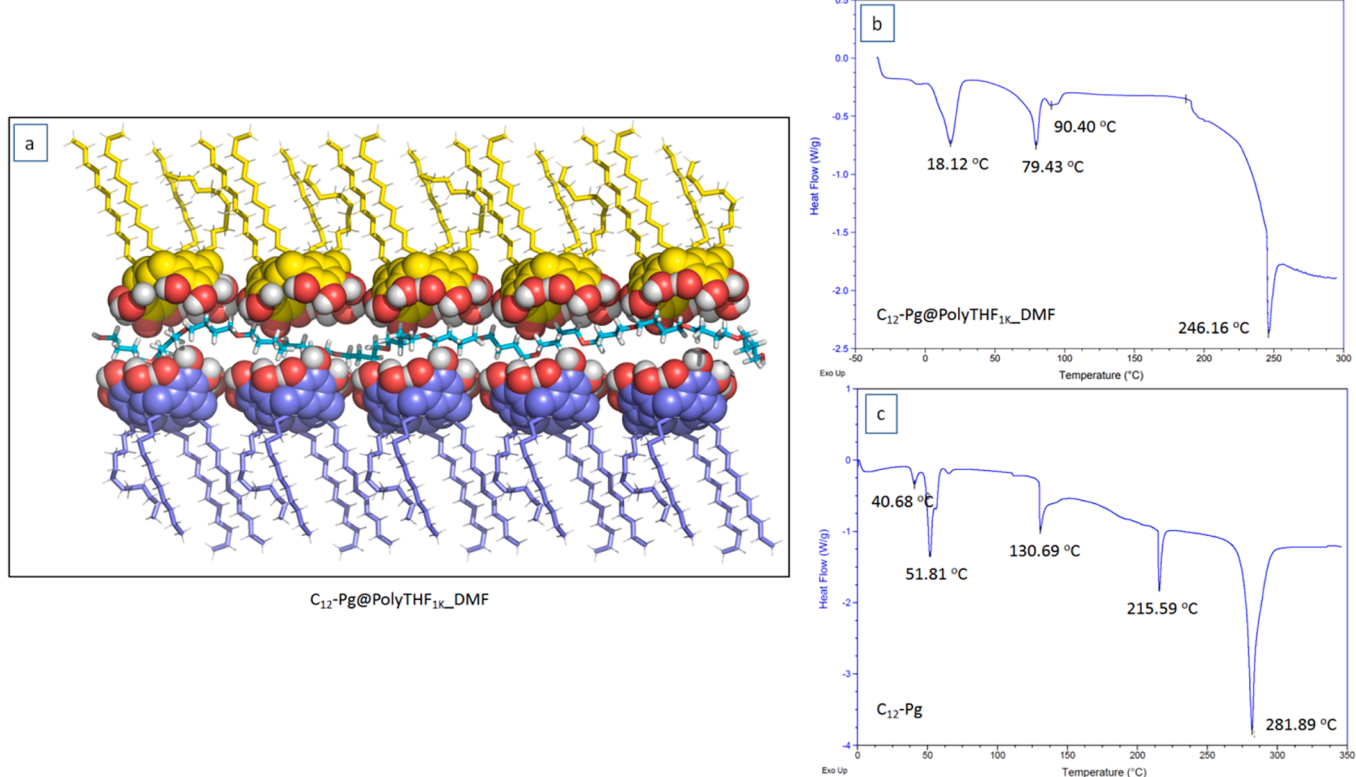


Fig. 5. Proposed model of $\text{C}_{12}\text{-Pg(bilayer)@polyTHF}_{1000}$ (DMF) supramolecular arrangement (panel a, polyTHF₁₀₀₀ chain depicted in cyan color is positioned in between two layers of $\text{C}_{12}\text{-Pg}$ molecules facing each other with crowns shown in CPK format and radiating dodecyl side chains represented as sticks) and its respective DSC plot (panel b) vs. starting material – $\text{C}_{12}\text{-Pg}$ bilayer motif DSC plot (panel c). (For interpretation of the references to color in this figure legend, the reader is referred to the web version of this article.)

can be easily seen in the respective DSC plots (Figs. S44–S57). Another plausible explanation for multiple DSC maxima is an extensive hydrogen bonding between polyTHF and the respective pyrogallol[4]arene macrocycle leading to semi-solids of different composition. Shown below is hypothetical model of C₁₂-Pg compound with lodged in polyTHF₁₀₀₀ chain (Fig. 5a). It is derived from an actual X-ray structure of C₁₂-Pg bilayer supramolecular arrangement obtained in DMF with an overlay of polyTHF chain to represent plausible mode of interaction between C₁₂-Pg crowns and a macromolecule. As it may be seen in the panels b and c of the Fig. 5, endothermic peaks corresponding to the blend C₁₂-Pg(bilayer)@polyTHF₁₀₀₀ (DMF) are markedly different from the ones observed for both starting materials, i.e., C-dodecylpyrogallol[4]arene as well as polyTHF₁₀₀₀ (Fig. S56, panel c), which indicated apparent changes in supramolecular organization upon blend preparation. More DSC data of the various polyTHF supramolecular blends formed in DMF are summarized in ESI (Figs. S46, S47). Similar trend was found for C-cyclohexylpyrogallol[4]arene based mixtures (Figs. S53, S54) and for a model C-propylpyrogallol[4]arene derived blends (Fig. S55). Importantly, short time exposure to 100 °C led to some changes in case of C₁₂-Pg(bilayer)@polyTHF₂₉₀₀ (DMF) supramolecular compound (Fig. S47), thus, suggesting their temperature dependent dynamic behavior. Presumably, C₁₂-Pg(caps.)@polyTHF blends prepared in PhNO₂/MeOH (10:1, v) solvent mixture may show somewhat high level of organization compared to the corresponding C₁₂-Pg bilayer arrangements obtained in DMF, EtOAc, and EtOAc/MeCN (1:1, v) solvent mixtures. Thus, slightly different behaviors (endothermic peaks) were observed (Figs. S44, S45, Table S3). Again, multiple endothermic peaks in the examined DSC plots may correspond to different composition of C-substituted pyrogallol[4] arene solvates having either “bilayer” lamellar organization or nanocapsules surrounded by disoriented polyTHF chains, thus forming a supramolecular polymeric material. The latter cannot be easily differentiated by using GPC analysis (Figs. S58, S59) implying that this method is not suitable for H-bonded supramolecular compounds.

Generally, no outstanding features attributed to either bilayer or nanocapsule based blends can be identified in either TGA or DSC plots due to the apparent thermal degradation at high temperatures.

For simplicity, we used a 1:1 ratio in weight between the examined pyrogallol[4]arene and polyTHF to avoid formation of slurries with one component greatly prevailing over another one in the mixture as a result of their molecular weight difference, so macroscopic properties of the blend, e.g., viscosity, would be mostly predetermined by an excess component. However, we realize that various ratios may be employed to prepare corresponding Pg@polyTHF blends. Hence, we recorded ¹H NMR spectra of a limited series of C₃-Pg@polyTHF₂₅₀ compounds of 1:1, 2:3, and 3:2 M ratio (Figs. S60–S64). We infer that all the solution findings may be irrelevant in the context of current work focused on semi-solids and assessment of their macroscopic properties. Overall, all the ¹H NMR data unequivocally supports the presence of both starting components and their supramolecular assemblies in solution, however, the latter is not clear enough to be convincing as no direct evidence found for interaction between model C₃-Pg and polyTHF₂₅₀ chains. A plausible, but speculative, explanation is that many of host-guest type complexes may co-exist in the solution with overlapping peaks of 1,4-butanediol segments at around 3.3 ppm when monomer units are surrounded by randomly oriented polyTHF chains with encapsulated solvents. Accordingly, performed dynamic viscosity measurements for an exemplary C₁₂-Pg@polyTHF_{250,650,1000,2000}(DMF) blends suggested non-linear dependence of complex viscosity on temperature unlike seen for the corresponding starting polyTHF materials (Figs. S65–S72). This may be due to the extensive clustering and material aggregation leading to the inhomogeneity in polymer networks that may influence the macroscopic properties and crystallization behaviour of the latter, i.e., melting temperature and crystallinity [50].

Thus, an addition of the specific supramolecular organizations of C-substituted pyrogallol[4]arenes, i.e., either in a form of bilayer or hexameric nanocapsule, to commercially available polyTHFs afforded

supramolecular polymer materials with enhanced viscosity, possibly, due to an extensive hydrogen bonding reminiscent of the patterns discovered by X-ray analysis for C-dodecyl- and C-cyclohexylpyrogallol [4]arenes. All aforementioned determinative factors, such as macrocycle and polyTHF chain length, solvent, stoichiometric ratio of components, which impact self-assembly when preparing semi-solids, should not be underestimated.

Conclusions

In the present work, a small series of C-alkylpyrogallol[4]arenes that hold potential to form supramolecular aggregates with commercially available polytetrahydrofurans has been prepared and their semi-solid mixtures were characterized by means of FT-IR, TGA, and DSC techniques as well as by viscosity measurements. Single crystal X-ray structures provided valuable insight into supramolecular organization of examined macrocycles and revealed common H-bonded patterns which included bridging solvent molecules and interdigitating side chains in both multilayer and capsular motifs. The importance of these studies is that C-alkylpyrogallol[4]arenes either in a form of bilayer or nanocapsule may be used to strengthen interactions between neighboring polyTHF chains and, consequently, can lead to the formation of transient supramolecular networks with an enhanced viscosity. We infer that pyrogallol[4]arene molecular structure as well as its supramolecular organization governed by solvent choice are the key factors to determine macroscopic properties of the supramolecular polymer blends at particular temperature. Viscosity determinations for C₁₂-Pg@polyTHF blends showed deviation from linear polymer dynamics observed for starting polyTHF materials and overall analytical data are suggestive of a plausible disintegration of the bilayer arrangements to the discrete pyrogallol[4]arene monomer at elevated temperatures. Except some outliers, shear viscosity data seemed to correlate with polyTHF molecular weight. A clear understanding of the mechanism of pyrogallol[4] arene induced polyTHF self-assembly in a slurry is beneficial for a design of industrially relevant polyTHF adhesive materials with tunable viscoelastic properties.

CRediT authorship contribution statement

Oleg Andrew Kulikov: Writing – review & editing, Writing – original draft, Supervision, Resources, Methodology, Conceptualization. **Arshad Mehmood:** Software, Data curation. **Sergey Vodzinsky:** Visualization, Resources, Investigation.

Declaration of competing interest

The authors declare that they have no known competing financial interests or personal relationships that could have appeared to influence the work reported in this paper.

Appendix A. Supplementary data

Supplementary data to this article can be found online at <https://doi.org/10.1016/j.rechem.2024.101804>.

References

- [1] H. Kumari, C.A. Deakyne, J.L. Atwood, Acc. Chem. Res. 47 (2014) 3080.
- [2] V.S. Sharma, V.K. Vishwakarma, P.S. Shrivastav, A.A. Sudhakar, A.S. Sharma, P. A. Shah, ACS Omega 7 (2022) 45752.
- [3] L. Avram, Y. Cohen, J. Rebek Jr., Chem. Commun. 47 (2011) 5368.
- [4] M. Chwastek, P. Cmoch, A. Szumna, J. Am. Chem. Soc. 144 (2022) 5350.
- [5] A. Rosu-Finsen, Nat. Rev. Chem. 7 (2023) 532.
- [6] R. Capelli, G.M. Piccini, J. Phys. Chem. C 128 (2024) 635.
- [7] J. Jumina, Y. Priastomo, H.R. Setiawan, Y.S. Mutmainah, K. Kurniawan, J.E. Ohto, Chem. Eng. (2020) 103971.
- [8] J. Jumina, D. Siswanta, A.K. Zulkarnain, S. Triono, P. Priatmoko, E. Yuanita, N. Fatmasari, I. Nursalim, Indones. J. Chem. 19 (2019) 273.

- [9] C. Ji, S. Liu, K. Su, E.M. El-Sayed, H. Liu, W. Wang, F. Qiu, X. Li, D. Yuan, A.C. S. Mater, Lett. 3 (2021) 1315.
- [10] H.R. Jumina, S. Setiawan, Y.S. Triono, Y. Kurniawan, D. Priastomo, A.K. Siswanta, N. Zulkarnain, Kumar Bull. Chem. Soc. Jpn. 93 (2020) 252.
- [11] J.L. Casas-Hinestrosa, A. Cifuentes, E. Ibáñez, M. Maldonado, J. Mol. Struct. 1210 (2020) 128063.
- [12] V. Posligha, A.S. Urbina, L. Rincon, J.-C. Soetens, M.A. Mendez, C.H. Zambrano, F. J. Torres, Comput. Theor. Chem. 1073 (2015) 75.
- [13] R.R. Putri, H.D. Pranowo, Y.S. Kurniawan, H.A. Fatimi, J. Jumina, Indones. J. Chem. 23 (2023) 1032.
- [14] S. Negin, R. Li, O.V. Kulikov, M.M. Daschbach, G.W. Gokel, Inorganica Chim. Acta 417 (2014) 177.
- [15] O.V. Kulikov, R. Li, G.W. Gokel, Angew. Chem. Int. Ed. 48 (2009) 375.
- [16] G.W. Gokel, S. Negin, Acc. Chem. Res. 46 (2013) 2824.
- [17] S. Negin, M.M. Daschbach, O.V. Kulikov, N. Rath, G.W. Gokel, J. Am. Chem. Soc. 133 (2011) 3234.
- [18] H. Kumari, L. Erra, A.C. Webb, P. Bhatt, C.L. Barnes, C.A. Deakyne, J.E. Adams, L. J. Barbour, J.L. Atwood, J. Am. Chem. Soc. 135 (2013) 16963.
- [19] C. Capacchione, D. Picariello, P.D. Sala, C. Talotta, P. Neri, I. Bruno, A. Pauciulo, A. R. Bartiromo, R. Glubizzi, C. Gaeta, ACS Omega 5 (2020) 18218.
- [20] T. Krause, M. Gruner, D. Kuckling, W.D. Habicher, Tetrahedron Lett. 45 (2004) 9635.
- [21] G.W. Gokel, S. Negin, Adv. Drug Deliv. Rev. 64 (2012) 784.
- [22] S. Negin, M.R. Gokel, M.B. Patel, S.L. Sedinkin, D.C. Osborn, G.W. Gokel, RSC Adv. 5 (2015) 8088.
- [23] P. Ziaja, K. Jodko-Piorecka, R. Kuzmicz, G. Litwinienko, Polym. Chem. 3 (2012) 93.
- [24] Q. Zhang, L. Catti, K. Tiefenbacher, Acc. Chem. Res. 51 (2018) 2107.
- [25] V. Iuliano, P.D. Sala, C. Talotta, M.D. Rosa, A. Soriente, C. Gaeta, P. Neri, Curr. Opin. Colloid Interface Sci. 65 (2023) 101692.
- [26] T. Klucznik, L.-D. Syntirvanis, S. Baš, B. Mikulak-Klucznik, M. Moskal, S. Szymkuć, J. Mlynarski, L. Gadina, W. Beker, M.D. Burke, K. Tiefenbacher, B.A. Grzybowski, Nature 625 (2024) 508.
- [27] L.-D. Syntirvanis, I. Némethová, D. Schmid, S. Levi, A. Prescimone, F. Bissegger, D. T. Major, K. Tiefenbacher, J. Am. Chem. Soc. 142 (2020) 5894.
- [28] Q. Zhang, K. Tiefenbacher, Nature Chem. 7 (2015) 197.
- [29] I. Cornu, L.-D. Syntirvanis, K. Tiefenbacher, Nat. Protoc. 19 (2024) 313.
- [30] P.L. Manna, C. Talotta, C. Gaeta, Y. Cohen, S. Slovak, A. Rescifina, P.D. Sala, M. D. Rosa, A. Soriente, P. Neri, Org. Chem. Front. 9 (2022) 2453.
- [31] S. Slovak, T. Salem, I. Horin, L. Avram, Y. Cohen, Org. Chem. Front. 11 (2024) 3294.
- [32] E.R. Abdurakhmanova, D. Mondal, H. Jedrzejewska, P. Cmoch, O. Danylyuk, M. J. Chmielewski, A. Szumna, Chem 10 (2024) 1635.
- [33] L. Shao, H. Zhang, X. He, B. Hua, X. Hu, C. Wan, S.P. Kelley, J.L. Atwood, J. Am. Chem. Soc. 143 (2021) 693.
- [34] H.-J. Buschmann, E. Schoillmeyer, J. Adhes. Sci. Technol. 24 (2010) 113.
- [35] K. Utaloff, M.H. Kothmann, M. Ciesielski, M. Döring, T. Neumeyer, V. Altstädt, I. Gorman, M. Henningsen, Polym. Eng. Sci. 59 (2018) 86.
- [36] D. Kim, D.G. Lee, J.C. Kim, C.S. Lim, N.S. Kong, J.H. Kim, H.W. Jung, S.M. Noh, Y. I. Park, Int. J. Adhes. Adhes. 74 (2017) 21.
- [37] K. Öjelund, T. Loontjens, P. Steeman, A. Palmans, F. Maurer, Macromol. Chem. Phys. 204 (2003) 52.
- [38] P. Shokrollahi, Iran. Polym. J. 19 (2010) 65.
- [39] M. Golkaram, L. Boetje, J. Dong, L.E.A. Suarez, C. Fodor, D. Maniar, E. van Ruymbeke, S. Faraji, G. Portale, K. Loos, ACS Omega 4 (2019) 16481.
- [40] M. Kohga, T. Naya, S. Shioya, J. Appl. Polym. Sci. 128 (2013) 2089.
- [41] O. Kulikov, S. Negin, N.P. Rath, G.W. Gokel, Supramol. Chem. 26 (2014) 506.
- [42] O. Kulikov, N. Rath, D. Zhou, I. Carasel, G. Gokel, New J. Chem. 33 (2009) 1563.
- [43] X. Zhu, T. Bai, Z. Wang, J. Liu, X. Min, T. Wang, W. Zhang, X. Fan, Polymers 11 (2019) 583.
- [44] S.J. Dalgarno, N.P. Power, J.E. Warren, J.L. Atwood, Chem. Commun. (2008) 1539.
- [45] S.A.M. Ali, D.J. Hourston, J. Appl. Polym. Sci. 43 (1991) 1503.
- [46] N. Howard, M.B. Huglin, R.W. Richards, J. Appl. Polym. Sci. 16 (1972) 1525.
- [47] J.L. Atwood, L.J. Barbour, A. Jerga, Chem. Commun. (2001) 2376.
- [48] S.N. Journey, K.L. Teppang, C.A. Garcia, S.A. Brim, D. Onofrei, J.B. Addison, G. P. Holland, B.W. Purse, Chem. Sci. 8 (2017) 7737.
- [49] M.M. Daschbach, O.V. Kulikov, E.F. Long, G.W. Gokel, Chem. Eur. J. 17 (2011) 8913.
- [50] R. Guo, K.I. Jacob, Polymer 55 (2014) 4468.